

Numerical investigation of sensible thermal energy storage in high temperature solar systems

A. Andreozzi¹, N. Bianco¹, O. Manca², S. Nardini² & V. Naso¹

¹DETEC – Università degli Studi di Napoli Federico II, Italy

²DIAM – Seconda Università degli Studi di Napoli, Aversa (CE), Italy

Abstract

A study on sensible thermal energy storage (TES) for high temperature solar systems is numerically accomplished. The high temperature TES is cylindrical, the fluid and the solid thermo-physical properties are temperature independent and the radiation heat transfer mechanism is neglected. A parametric analysis is carried out. The commercial CFD Fluent code is used to solve the governing equations in the transient regime. Numerical simulations are carried out at different mass velocity values of the heat-carrying fluid and porosity of the storage medium. The results show the effects of the porosity and of the working fluid mass velocity on the stored thermal energy and on the storage time.

Keywords: solar energy, sensible thermal energy storage, numerical analysis.

1 Introduction

Thermal energy storages (TESs) are employed in many solar thermal plants in order to ensure the continuity in energy supply and minimize instability. Moreover, the use of TES for thermal applications, such as space and water heating, cooling and air-conditioning, has recently received attention [1–4]. The storage purpose is twofold: to increase the value of the power generated by strongly reducing its randomness and to improve the plant economics by using the available hardware for more hours a year. Recent concentrating solar plant projects incorporate heat storage that allows the system to operate for some 6–12 hours in the absence of solar irradiance [5].



Three types of TES systems are, generally, employed in high temperature applications: latent heat storage systems, molten salt storage systems and sensible heat storage systems. Cost effective systems demand the utilisation of inexpensive storage materials, which usually exhibit a low thermal conductivity. Essential for the successful development of a storage system is the sufficient heat transfer between the fluid and the storage material. Recently, a high temperature TES was studied by a lab-scale cylindrical storage tank experiment [6]. A heat exchanger of TES was used for separating two fluids: the storage medium and the heat transfer fluid. A multi-tank sensible-heat storage system for storing thermal energy, with a two-tanks molten salt system, was proposed in [7].

In a high concentrating solar receiver, the temperature reaches values in the range from 800 °C to 1800 °C and the fluid employed in the plant is often a gas, such as air. In air based solar energy utilization systems, storage of hot air is not possible due its low density. A denser medium is required for storage of thermal energy. In sensible TES, energy is stored by changing the temperature of a storage medium, such as water, oil, rock beds, bricks, sand or soil. The amount of energy input to TES by a sensible heat device is proportional to the difference between the final and initial temperatures of the storage medium, its mass and its specific heat. Each medium has its own advantages and disadvantages. Packed bed generally represents the most suitable energy storage unit for air based solar energy systems as mentioned in [8]. An extensive literature review of research work was presented in [9,10] and, more recently, in [11,12].

Several investigations on fixed bed energy storage use the model originally developed by Schumann [13]. This is a one dimensional two-phase transient model that enables the prediction of the axial and temporal distribution of the solid and fluid temperatures. Experiments using steel spheres to determine the heat transfer coefficient between the fluid and solid for air as the working fluid were accomplished in [14]. A modified version of Schumann's model was employed in [15] to solve the model equations using gas as the working fluid. A model with the fixed bed divided into two regions, one near the wall with high void fraction and the other in the bed central region was studied in [16]. The results and method given in [15] were employed in [16] to evaluate the temperature distribution and in [17] to verify high computational times when the ratio of the specific heat of the solid to the specific heat of the fluid was high. Investigations concerning the effects of the radial and axial dispersion in the bed were presented in [18,19]. How a single phase model can be derived from the continuous solid phase model was demonstrated in [20]. A storage unit of the fixed type using Schumann's model, including possible variations in the fluid inlet temperature, was modelled in [21].

It was found that the optimization of the packed bed design should aim at maximizing the ratio of total energy availability to total pumping energy, which increases when the size of the material elements increases [22]. However, thermal performance of the system may deteriorate due to the smaller area of contact available for heat transfer [23].

A numerical study on packed bed thermal models, suitable for sensible and latent heat thermal storage systems, was accomplished in [11]. An experimental



investigation on the effect of the system and operating parameters on heat transfer and the pressure drop characteristics of a packed bed solar energy storage system with large sized elements of storage material was conducted in [12]. Solid media sensible heat storage materials were investigated in the experimental study reported in [24]. A thermodynamic procedure to analyze the energy and exergy balances of a rock bed thermal storage system was presented in [25]. A numerical investigation on the sensitivity of the long-term performance simulations of solar energy systems to the degree of stratification in both liquid and packed bed storage units was carried out in [26].

In this paper a high temperature sensible TES is numerically analyzed and a parametric analysis is accomplished. In the formulation of the model it is assumed that the system geometry is cylindrical, the fluid and the solid thermo-physical properties are temperature independent, and the radiation heat transfer mechanism is neglected. The commercial CFD Fluent code is used to solve the governing equations in the transient regime. Numerical simulations are carried out at different mass velocities of the heat-carrying fluid and porosity of the storage medium. The results show the effects of the porosity and of the working fluid mass velocity on the stored thermal energy and on the storage time.

2 Mathematical description and numerical procedure

The proposed prototype of high temperature sensible TES is a cylinder whose diameter is equal to 0.60 m and height is equal to 1.0 m. The storage material is steel and it is assumed to be a porous medium. The heat-carrying fluid is air. The thermo-physical properties of the steel and the air, reported in Tables 1 and 2, are temperature independent. The radiation heat transfer mechanism is neglected.

Table 1: Steel thermo-physical properties.

Property	
c [J/kg K]	502.48
ρ [kg/m ³]	8030
k [W/m K]	16.27

Table 2: Air thermo-physical properties.

Property	
c [J/kg K]	1006.43
ρ [kg/m ³]	1.225
k [W/m K]	0.0242



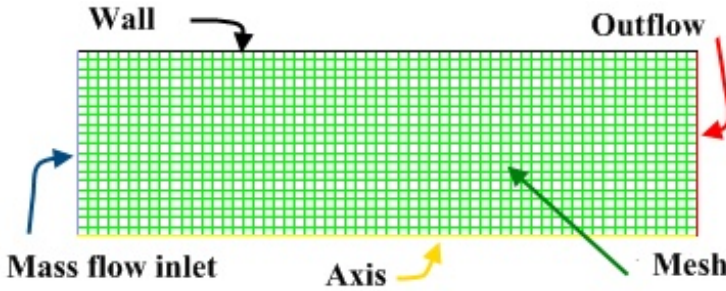


Figure 1: Computational domain with imposed boundary conditions.

Thanks to the axisymmetry of the physical model, a two-dimensional analysis was carried out. The employed computational domain is sketched in Fig.1, where the imposed boundary conditions are reported.

The temperature of the hot air entering the channel, T_{in} , is equal to 1473 K.

The commercial CFD code Fluent [27] was employed to solve the governing equations in transient and laminar regime. A rectangular shape mesh with 76800 cells has been employed. The initial temperature of the solid elements and of the heat-carrying fluid is assumed to be equal to 1073 K. Air is the heat-carrying fluid, that is assumed to be an incompressible ideal gas.

Numerical simulations are carried out for different mass velocity values. The mass velocity, G , is the ratio of the module mass flow rate, \dot{m} , to the free flow area of the storage module cross section S , that can be expressed as the product of the frontal area of the module and its porosity

$$G = \frac{\dot{m}}{S} \quad (1)$$

For assigned G , different porosity values were considered. Results are given in terms of stored thermal energy in porous medium after the considered time interval, Q_{stored} , as a function of time. The stored thermal energy is evaluated as

$$Q_{stored} = \rho_{eff} c_{eff} \left[\int_V \bar{T} dV - T_i V \right] \quad (2)$$

where $V = 0.283 \text{ m}^3$ and $T_i = 1073 \text{ K}$. ρ_{eff} and c_{eff} are evaluated by:

$$\rho_{eff} = \varepsilon \rho_f + (1 - \varepsilon) \rho_s ; \quad c_{eff} = \varepsilon c_f + (1 - \varepsilon) c_s \quad (3)$$

In Table 3, the effective density and specific heat values, evaluated for different porosity values, are reported. The viscous and inertial resistance coefficients, $1/\alpha$ and C_2 respectively, depend on G and ε . In Table 4 they are reported for different porosity values.

A grid dependence analysis was obtained for $G=0.245 \text{ kg/m}^2\text{s}$, $T_i=1200 \text{ K}$, $T_{amb}=300 \text{ K}$, $\varepsilon=0.40$, $1/\alpha=6.00 \times 10^5 \text{ m}^{-2}$ and $C_2=1312.5 \text{ m}^{-1}$. Six meshes were considered: 10×30 , 20×60 , 40×120 , 80×240 , 160×480 and 320×960 . The comparison among results allows one to employ in the simulations the mesh 160×480 as the more appropriate to obtain an adequate accuracy with a convenient computational time. A similar analysis was carried out also for different time steps. The most advantageous time step was equal to 5 s.

The converging criteria were 10^{-3} for the residuals of the velocity components and 10^{-6} for the residuals of the energy.

Table 3: Effective density and specific heat of porous medium for different porosity values.

ε	$\rho_{eff} (\text{kg} / \text{m}^3)$	$c_{eff} (\text{J} / \text{kg} \text{ K})$
0.20	6424.20	603.27
0.30	5621.30	653.60
0.35	5219.93	678.86
0.40	4818.49	729.18
0.45	4417.05	725.25
0.50	4015.61	754.45
0.60	3212.70	804.85

Table 4: Viscous and inertial resistance coefficients for different porosity values.

ε	$1/\alpha (\text{m}^{-2})$	$C_2 (\text{m}^{-1})$
0.20	3846153	14000
0.30	1307189	3629
0.35	827814	2122.4
0.40	600000	1312.5
0.45	358551	845
0.50	240030	280
0.60	107526	259



3 Results and discussion

Numerical simulations are carried out at the following mass velocity values: 0.20 kg/m²s, 0.30 kg/m²s and 0.40 kg/m²s and for an inlet temperature of the air equal to 1473 K. The porosity ϵ varies from 0.20 to 0.60.

The stored thermal energy for a mass velocity value $G=0.20$ kg/m²s and for different porosity values is reported in Fig.2. The profiles trends show that at initial time the stored energy is higher for the higher ϵ value and they present an inversion at different time increasing the porosity value. Moreover, increasing the porosity determines a substantial decrease of the stored thermal energy in the long time. At each porosity the stored thermal energy reaches an asymptotic value, which indicates the thermal saturation of the reservoir. The time at which the thermal saturation is reached increases with decreasing porosity due to the increase in the thermal capacity of the reservoir. The lower thermal inertia causes a temperature increase in less time and a smaller thermal capacity, which determines the heat storage saturation in less time, too. The stored thermal energy values are reported in Table 5 for the first eight hours of computational simulation. The choice of this time period allows one to compare this values sequence with different porosity. For $\epsilon \geq 0.45$ and after 4 hours, thermal energy stored reaches the 95% of the maximum stored thermal energy value, which is attained after 8 hours. Moreover, the previous observation is confirmed and the best condition for the thermal energy storage is that obtained for a porosity equal to 0.40 after three hours, with $Q_{\text{stored}}=3.43 \times 10^5$ kJ.

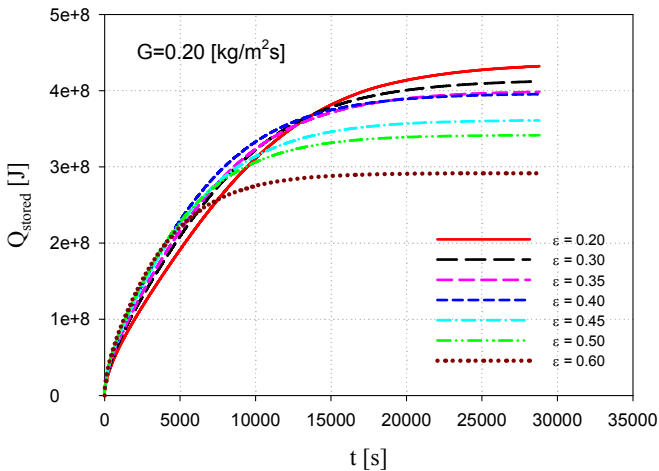


Figure 2: Stored thermal energy vs. time for $G=0.20$ kg/m²s and various porosity values.

Table 5: Stored thermal energy values for the first eight hours of computational simulation and $G=0.20 \text{ kg/m}^2\text{s}$.

ε	Q_{stored} [kJ] 3600 s	Q_{stored} [kJ] 7200 s	Q_{stored} [kJ] 10800 s	Q_{stored} [kJ] 14400 s
0.20	150545	249630	325596	375233
0.30	165968	266798	334424	373683
0.35	172768	272400	334322	367535
0.40	185031	285228	342594	371606
0.45	182430	274022	321423	343735
0.50	186881	272402	312521	329944
0.60	187578	253941	278580	287312
ε	Q_{stored} [kJ] 18000 s	Q_{stored} [kJ] 21600 s	Q_{stored} [kJ] 25200 s	Q_{stored} [kJ] 28800 s
0.20	404451	419274	427647	432088
0.30	394171	404327	409534	412137
0.35	384404	392709	396618	398400
0.40	384977	391266	394156	395447
0.45	353897	358319	360177	360911
0.50	337129	339952	341093	341539
0.60	290290	291261	291579	291681

Increasing the mass velocity value, $G=0.30 \text{ kg/m}^2\text{s}$, in Fig. 3, the differences with respect to the previous case are significant in terms of thermal saturation time. In fact, for this configuration, the profile of the stored thermal energy for a porosity value equal to 0.60 shows the asymptotic value after about 10000 s whereas in the first case this value was about 15000 s. This is due to an increase in the convective heat transfer between the air and the porous medium. This is also evident in Table 6 where the stored thermal energy values are reported for the first eight hours of computational simulation. In this case for a porosity equal to 0.40 a $Q_{\text{stored}}=3.41 \times 10^5 \text{ kJ}$, very close to the previous value for $G=0.20 \text{ kg/m}^2\text{s}$, is attained after 2 hours. It is about the 86% of the saturation value ($Q_{\text{max}}=3.96 \times 10^5 \text{ kJ}$). Then the higher value of G determines a lower time needed to reach a good thermal storage level.

The variation in the stored thermal energy profiles is more marked when the mass velocity value is varied from $G=0.30 \text{ kg/m}^2\text{s}$ to $G=0.40 \text{ kg/m}^2\text{s}$, as it is observed in Fig 4. For the lowest porosity values the profiles still show an increasing trend with higher stored thermal energy values, whereas for the higher porosity values a sudden increase in the thermal energy stored in the solid medium is observed. It is necessary to underline a progressive change in the material behaviour at increasing mass velocity values, the larger the porosity the larger the change. A reduction in the time necessary to reach the steady state, passing from about 10000 s for $G=0.30 \text{ kg/m}^2\text{s}$ to about 7500 s for $G=0.40 \text{ kg/m}^2\text{s}$, at $\varepsilon=0.60$, is also observed, but with a considerable decrease in the inversion time. The value of this time between $\varepsilon=0.20$ and $\varepsilon=0.60$ changes

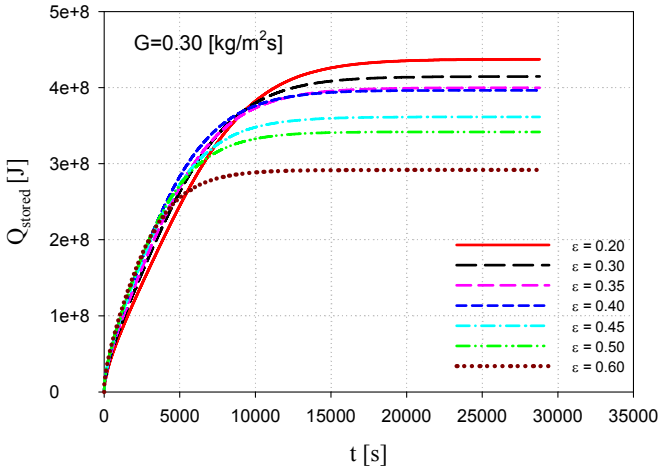


Figure 3: Stored thermal energy vs. time for $G=0.30 \text{ kg/m}^2\text{s}$ and various porosity values.

Table 6: Stored thermal energy values for the first eight hours of computational simulation and $G=0.30 \text{ kg/m}^2\text{s}$.

ϵ	$Q_{\text{stored}} \text{ [kJ]}$ 3600 s	$Q_{\text{stored}} \text{ [kJ]}$ 7200 s	$Q_{\text{stored}} \text{ [kJ]}$ 10800 s	$Q_{\text{stored}} \text{ [kJ]}$ 14400 s
0.20	188403	319531	393888	423381
0.30	206097	330770	387898	407012
0.35	213655	331778	379522	394244
0.40	227702	340926	381475	392818
0.45	223207	321104	351540	359157
0.50	226780	312389	335368	340527
0.60	222384	279047	289661	291420
ϵ	$Q_{\text{stored}} \text{ [kJ]}$ 18000 s	$Q_{\text{stored}} \text{ [kJ]}$ 21600 s	$Q_{\text{stored}} \text{ [kJ]}$ 25200 s	$Q_{\text{stored}} \text{ [kJ]}$ 28800 s
0.20	433180	436145	436926	437152
0.30	412586	414029	414390	414483
0.35	398396	399466	399721	399777
0.40	395587	396218	396362	396393
0.45	360943	361325	361401	361414
0.50	341565	341757	341792	341798
0.60	291684	291720	291725	291726

from about 7000 s for $G=0.20 \text{ kg/m}^2\text{s}$ to about 4000 s for $G=0.40 \text{ kg/m}^2\text{s}$. For this configuration the best condition for the thermal energy storage is obtained for $\epsilon=0.20$, as observed in Table 7. In fact, after 2 hours the highest Q_{stored} value is equal to $3.76 \times 10^5 \text{ kJ}$ for $\epsilon=0.20$ and it is about 86% of Q_{max} at this porosity.



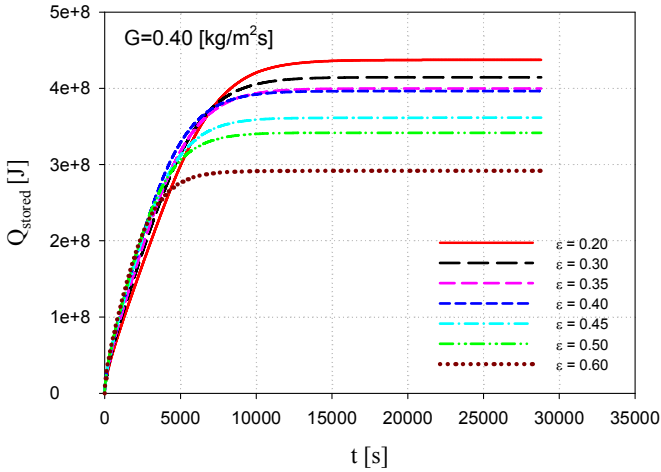


Figure 4: Stored thermal energy vs. time for $G=0.40 \text{ kg/m}^2\text{s}$ and various porosity values.

Table 7: Stored thermal energy values for the first eight hours of computational simulation and $G=0.40 \text{ kg/m}^2\text{s}$.

ϵ	Q_{stored} [kJ] 3600 s	Q_{stored} [kJ] 7200 s	Q_{stored} [kJ] 10800 s	Q_{stored} [kJ] 14400 s
0.20	228993	376386	425931	435473
0.30	248076	376379	408565	413761
0.35	255517	371042	395671	399281
0.40	270274	374796	393724	396128
0.45	262398	347110	359920	361273
0.50	263517	332258	340914	341730
0.60	250651	288679	291539	291716
ϵ	Q_{stored} [kJ] 18000 s	Q_{stored} [kJ] 21600 s	Q_{stored} [kJ] 25200 s	Q_{stored} [kJ] 28800 s
0.20	437005	437213	437237	437240
0.30	414430	414505	414512	414513
0.35	399736	399787	399791	399792
0.40	396377	396399	396401	396401
0.45	361405	361416	361417	361417
0.50	341794	341799	341799	341799
0.60	291725	291725	291725	291725



4 Conclusions

A numerical investigation on thermal energy storage at high temperature was carried out. The storage is a component of a high temperature (>800 °C) thermal solar plant. The thermal storage was cylindrical, the storage medium was a solid and it was modelled as a porous medium. The transient regime analysis was accomplished in the heating phase of the thermal storage with different mass velocity and porosity values.

Results showed that, for the considered parameter values, thermal saturation of the TES was attained after eight hours for all considered porosity values and the larger the mass velocity the lower the saturation time. For an assigned mass velocity value the larger the porosity the higher the stored thermal energy at initial time. After the inversion time the trend is the opposite, i.e., the larger the porosity the lower the maximum storage thermal energy, Q_{\max} . However, the best value of porosity to reach about 0.85 Q_{\max} in the lowest time is 0.40 for the lowest considered G values and 0.20 for the highest considered G values.

Acknowledgement

This work was supported by MIUR with Articolo 12 D. M. 593/2000 Grandi Laboratori "EliosLab".

Nomenclature

c	specific heat, $\text{J kg}^{-1} \text{K}^{-1}$	Greek symbols	
C_2	inertial resistance coefficient, m^{-1}	α^{-1}	viscous coefficient, m^{-2}
G	mass velocity, $\text{kg m}^{-2}\text{s}^{-1}$	ε	porosity
k	thermal conductivity, $\text{Wm}^{-1}\text{K}^{-1}$	ρ	density, kg m^{-3}
\dot{m}	mass flow rate, kg s^{-1}	Subscript	
Q	thermal energy, J	amb	ambient
Q_{stored}	stored thermal energy, J	eff	effective
S	free flow area of module storage cross section, m^2	f	fluid
t	time, s	i	initial
T	temperature, K	in	entering
V	volume, m^3	max	maximum value
		s	solid

References

- [1] Dincer, I. & Rosen, M., *Thermal energy storage: System and application*, John Wiley & Sons, 2002.



- [2] Paksoy, H. Ö., *Thermal energy storage for sustainable energy consumption: Fundamentals, Case studies and design*, Springer, 2007.
- [3] Beckmann, G. & Gilli, P.V., *Thermal energy storage: Basics, Design, Applications to power generation and heat supply*, Springer, 2002.
- [4] Sharma, A., Tyagi, V.V., Chen, C.R. & Buddhi, D., Review on thermal energy storage with phase change materials and applications, *Renewable and Sustainable Energy Reviews*, **13**, pp. 318-345, 2009.
- [5] Angelino, G. & Invernizzi, C., Binary conversion cycles for concentrating solar power technology, *Solar Energy*, **82** (7), pp. 637-647, 2008.
- [6] Vaivudh, S., Rakwichian, W. & Chindaruksa, S., Heat transfer of high thermal energy storage with heat exchanger for solar trough power plant, *Energy Conversion and Management*, **49**, pp. 3311–3317, 2008.
- [7] Salomoni, V. A., Majorana, C. E., Giannuzzi, G. M. & Miliozzi, A., Thermal-fluid flow within innovative heat storage concrete systems for solar power plants, *International Journal of Numerical Methods for Heat and Fluid Flow*, **18** (7-8), pp. 969-999, 2008.
- [8] Cautier, J. P. & Farber, E. A., Two applications of a numerical approach of heat transfer process within rock beds, *Solar Energy*, **29**, pp.451–462, 1982.
- [9] Barker, J. J., Heat transfer in packed beds, *Industrial & Engineering Chemistry*, **57**, pp. 43–51, 1965.
- [10] Balakrishnan, A., Pei, R. & David, C. T., Heat transfer in packed bed systems – a critical review, *Industrial and Engineering Chemistry, Process Design and Development*, **18**, pp.30–40, 1979.
- [11] Ismail, K. A. R. & Stuginsky, R. Jr., A parametric study on possible fixed bed models for pcm and sensible heat storage, *Applied Thermal Engineering*, **19**, pp.757–788, 1999.
- [12] Singh, R., Saini R. P. & Saini, J. S., Nusselt number and friction factor correlations for packed bed solar energy storage system having large sized elements of different shapes, *Solar Energy*, **80**, pp.760–771, 2006.
- [13] Schumann, T. E. W., Heat transfer: a liquid flowing through a porous prism, *J. Franklin Inst.*, **208**, pp.405–416, 1929.
- [14] Furnas, C. G., Heat transfer from a gas stream to a bed of broken solids II, *Industrial & Engineering Chemistry*, **22**, pp. 721-731, 1930.
- [15] Handley, D. & Heggs, P. J., The effect of thermal conductivity of the packing material on transient heat transfer in a fixed bed, *International Journal of Heat and Mass Transfer*, **12**, pp.549–570, 1969.
- [16] Gross, D. J., Hickox, C. E. & Hackett, C. E., Numerical simulation of dual-media thermal energy storage systems, *Trans. ASME, Journal of Solar Energy Engineering*, **102**, pp.287–297, 1980.
- [17] Beasley, D. E. & Clark, J. A., Transient response of a packed bed for thermal energy storage, *International Journal of Heat and Mass Transfer*, **27**, pp.1659–1699, 1984.
- [18] Gunn, D. J., Axial and radial dispersion in fixed beds, *Chemical Engineering Science*, **42**, pp. 363-373, 1987.



- [19] Gunn, D. J., Ahmed M. M. & Sabri, M. N., Radial heat transfer to fixed beds of particles, *Chemical Engineering Science*, **42**, pp.2163–2171, 1987.
- [20] Vortmeyer, D. & Schaefer, R. J., Equivalence of one and two-phase models for heat transfer processes in packed beds: one dimensional theory, *Chemical Engineering Science*, **29**, pp. 485–491, 1974.
- [21] Sowell, E. F. & Curry, R. L., A convolution model of the rock bed thermal storage units, *Solar Energy*, **24**, pp.441–449, 1980.
- [22] Torab, H. & Beasley, D. E., Optimization of packed bed thermal energy storage unit, *Journal of Solar Energy Engineering*, **109 (3)**, pp.170–175, 1987.
- [23] Sagara, K. & Nakahara, N., Thermal performance and pressure drop of packed beds with large storage materials, *Solar Energy*, **47 (3)**, pp.157–163, 1991.
- [24] Laing, D., Steinmann, W. D., Tamme, R. & Richter, C., Solid media thermal storage for parabolic trough power plants, *Solar Energy*, **80 (10)**, pp. 1283-1289, 1980.
- [25] Navarrete-González, J. J., Cervantes-de Gortari, J. G. & Torres-Reyes, E. Exergy analysis of a rock bed thermal storage system, *International Journal of Exergy*, **5 (1)**, pp. 18-30, 2008.
- [26] Arias, D. A., McMahan, A. C. & Klein, S. A., Sensitivity of long-term performance simulations of solar energy systems to the degree of stratification in the thermal storage unit, *International Journal of Energy Research*, **32 (3)**, pp. 242-254, 2008.
- [27] Fluent Incorporated, Fluent 6.2, User Manual, Lebanon, NH, 2005.

